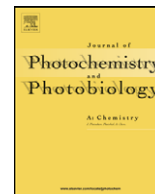




Contents lists available at ScienceDirect

Journal of Photochemistry and Photobiology A: Chemistry

journal homepage: www.elsevier.com/locate/jphotochem

Photodimers of *N*-alkyl-3,4-dimethylmaleimides—Product ratios and reaction mechanism

Xiuling Yu^a, Cathrin Corten^b, Helmut Görner^c, Thomas Wolff^{a,*}, Dirk Kuckling^b

^a *Physikalische Chemie, Technische Universität Dresden, D-01062 Dresden, Germany*

^b *Makromolekulare Chemie, Technische Universität Dresden, D-01062 Dresden, Germany*

^c *Max-Planck-Institut für Bioorganische Chemie, D-45413 Mülheim an der Ruhr, Germany*

ARTICLE INFO

Article history:

Received 18 January 2008

Received in revised form 15 February 2008

Accepted 18 February 2008

Available online 23 February 2008

Keywords:

Photodimerization

Photo-cross-linking

Flash photolysis

Triplet state

Reaction mechanism

Selectivity

ABSTRACT

The photodimerization of three *N*-alkyl-3,4-dimethylmaleimides (DMI) – frequently used to form crosslinks in polymers – was examined. *N*-Isobutyl-3,4-dimethylmaleimide, *N*-(2-acetamido)ethyl-3,4-dimethylmaleimide, *N*-(3-propionic acid)-3,4-dimethylmaleimide were studied by steady-state and time-resolved photolysis in various solvents. Unexpectedly, under all conditions a single-bonded dimer distinct from the well-known cyclobutane fused cyclic dimer was identified. Depending on the solvent the single-bonded dimer amounts to 5–50% of the product yield, allowing for considerable selectivity. Dimerization quantum yields, Φ_{dim} , range from 0.01 to 0.5. Results from time-resolved experiments establish the involvement of the triplet state in the photodimerization mechanism, the quantum yield of singlet molecular oxygen formation accounts for the Φ_{dim} values. Electron transfer and hydrogen abstraction reactions of DMI in polar and protic solvents, in contrast to *N*-alkylmaleimides, are inefficient processes.

© 2008 Elsevier B.V. All rights reserved.

1. Introduction

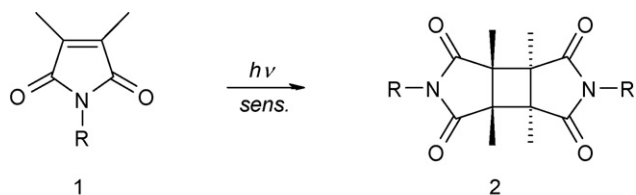
Photodimerization is a fundamental process and still the subject of numerous investigations [1,2]. For example, anthracenes [1], cinnamic acids [2a,3a] stilbenes [2b,c], and coumarins [2d–i] were investigated with respect to regio- and stereochemistry of photoproducts as well as solvent and temperature influences on product ratios [1c,d,2f,g]. The direct and sensitized photodimerization of DNA bases, such as thymine or uracil can be of biological importance [3]. Also, defined photo-cross-linking of polymers can be brought about via photodimerization of various chromophores [4].

The photodimerization of *N*-alkyl-3,4-dimethylmaleimides (DMI, **1**) was used for the generation of crosslinks in polymer systems [5,6] and for anchoring thin polymer layers on substrates [7–9]. It was reported [5–8] that DMIs form cyclic dimers with a transfused cyclobutane ring (**2** in Scheme 1). This was supported by an X-ray structure analysis of the dimer of *N*-ethyl-DMI [5a]. The triplet state was suggested as an intermediate in the reaction, since a triplet sensitizer was necessary [5]. The triplet energy is between 236 and 203 kJ mol⁻¹ since benzil as a sensitizer allowed the reaction whereas acridine orange did not [5a]. However,

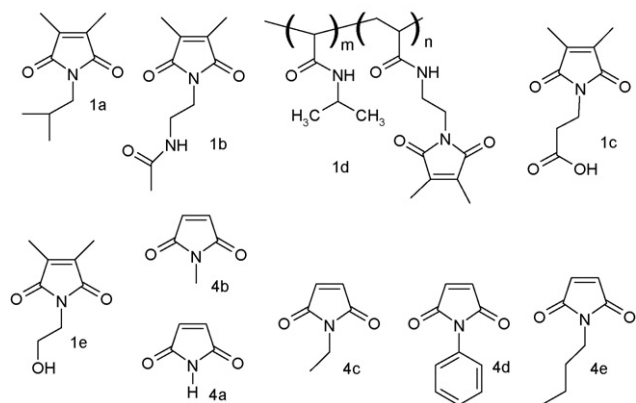
according to other papers [7,8c,d] a sensitizer is not necessary in solution. Very recently, a differently structured single-bonded photodimer **3** was reported to be formed in water but not in organic solvents [9]. A detailed preparative and mechanistic study on the photodimerization of DMI derivatives was not yet performed.

In contrast, the photochemistry of the parent compound maleimide, **4a**, and its *N*-alkylated derivatives was intensively investigated [10–20]. Single-bonded dimers were not reported. Radicals are formed and the question of biradical vs. ion radicals was discussed. *N*-Substituted maleimides undergo photoinduced copolymerization with electron donor monomers [14]. A free radical copolymerization of *N*-methylmaleimide, **4b**, and 2,3-dihydrofuran was initiated by their radical cations [16,20]. Based on a laser flash photolysis study with optical and conductometric detection **4a**, **4b** and *N*-ethylmaleimide, **4c**, are known to undergo protonation and dimerization in the triplet state [18]. The quantum yield of intersystem crossing (Φ_{isc}) of **4a** is low: $\Phi_{\text{isc}}=0.03$ in aqueous solution [19,17]. In a low temperature EPR study it has been shown that the polymerization of **4a** is initiated by monomer radical cations [16]. The laser flash photolysis studies were extended to *N*-phenylmaleimide [12,13] and bismaleimides [13]. As sensitizer for *N*-alkylmaleimides [16] and *N*-phenylmaleimides [15], **4d**, benzophenone was applied. For *N*-butylmaleimide, **4e**, at 1 mM in dichloromethane, a quantum yield of dimerization (Φ_{dim}) of 0.06 has been reported [11]. Maleimides were considered as electron-transfer photoinitiators in polymerizations [17].

* Corresponding author. Tel.: +49 351 46333633; fax: +49 351 46333391.
E-mail address: thomas.wolff@chemie.tu-dresden.de (T. Wolff).

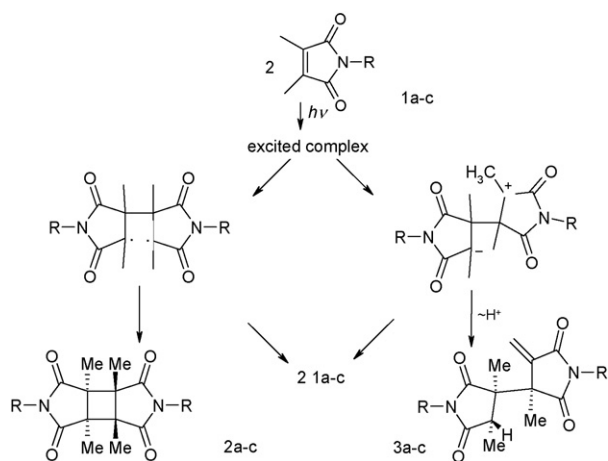


Scheme 1. Photodimerization of *N*-alkyldimethylmaleimides as reported [5–8].



Scheme 2. Compounds investigated (**1a–c** in preparative, **1a–d** and **4a, 4b** in flash experiments) or discussed (**1e, 4c–e**).

Here the photochemistry of *N*-isobutyl-3,4-dimethylmaleimide, **1a**, *N*-(2-acetamido)ethyl-3,4-dimethylmaleimide, **1b**, *N*-(3-propionic acid)-3,4-dimethylmaleimide, **1c**, was studied in order to clarify reaction mechanism, product ratios, and solvent effects in DMI and in polymers. Results from continuous irradiation and pulsed excitation are reported. For comparison, **4a** and a polymer with pendant DMI groups poly(*N*-isopropylacrylamide)-co-poly(acrylamide), **1d**, were included in the investigation, see **Scheme 2** for structural formulae. It will be shown that – besides the cyclic dimer **2** – in all DMI and in all solvents studied considerable amounts of a second single-bonded dimer **3** (**Scheme 3**) are formed.



For R see **Scheme 2**

Scheme 3. Mechanism of photodimerization of **1a–c** into **2a–c** and **3a–c**.

2. Results

2.1. Photodimer structures

The UV–vis absorption spectra of **1a** in cyclohexane, benzene and acetonitrile are shown in **Fig. 1** (inset). Variation of the concentration does not indicate any complex formation at higher concentrations. All spectra of **1a–1c** in organic solvents show no indication of any concentration effects of the ground state. The molar absorption coefficient of monomeric **1a** in acetonitrile is $\epsilon_{297} = 180 \text{ M}^{-1} \text{ cm}^{-1}$ (**Fig. 1**), that of **4d** is $\epsilon_{300} = 800 \text{ M}^{-1} \text{ cm}^{-1}$ [20]. **1a–c** in most organic solvents at room temperature did not show any emission of significance. The excited singlet state of **1a–1c** is therefore very short-lived.

Argon or air-saturated solutions of **1a–c** in various solvents in the presence and absence of sensitizers were irradiated at $\lambda > 300 \text{ nm}$ using a Xe–Hg lamp and a Duran glass filter. An example for the resulting absorption changes is shown in **Fig. 2b**. The major product in most cases is the transfused dimer **2**. Peaks in the NMR spectra of irradiated mixtures generally prove the formation of side products. HPLC analyses of irradiated solutions of **1a–1c**, however, revealed only one further product, **3** (cf. **Scheme 3**), with a slightly longer retention time (**Fig. 2a**). According to mass spectra, **3a** is also a dimer of **1a**. The NMR spectrum (see **Supporting material**) is in accordance with the single-bound dimer structure **3a** in **Scheme 3**. After separation and crystallization its structure was established by X-ray analysis (**Fig. 3b**) and is in accordance with the recently reported structure of the second photodimer of another DMI, *N*-(2-hydroxyethyl)-3,4-dimethylmaleimide **1e** [9]. X-ray crystal structures of the dimers **2a** and **2b** (**Fig. 3a** and c) corroborate the expectation from previous work [5a]. NMR-analyses of an irradiated solution of **1a** in methanol- d_1 , in D_2O and in acetonitrile- d_3 indicated that deuterium was not incorporated into the products or only to a minor extent, i.e. solvent protons are not necessarily involved in the formation of the two products. Above 280 nm **3a** only weakly absorbs whereas **2a** does not (**Fig. 1**). The molar absorption coefficient of **2a** is $\epsilon_{255} = 550 \text{ M}^{-1} \text{ cm}^{-1}$ and that of **3a** is $\epsilon_{245} = 740 \text{ M}^{-1} \text{ cm}^{-1}$.

2.2. Direct photoconversion and quantum yields

The photoconversion of **1a** into **2a** and **3a** has been followed by UV spectroscopy. Examples of plots of the photochemical conversion, pc, vs. the irradiation time are shown in **Fig. 4a** for **1a**

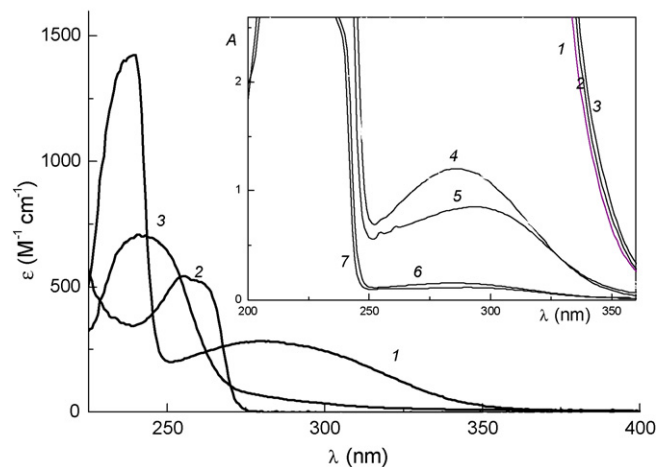


Fig. 1. UV-absorption spectra of air-saturated **1a** (**1**) and the two isolated products **2a** (**2**) and **3a** (**3**); inset: spectra in cyclohexane (1 cm: **1**, 1 mm: **4**, 0.1 mm: **6**), benzene (1 cm: **2**) and acetonitrile (1 cm: **3**, 1 mm: **5**, 0.1 mm: **7**).

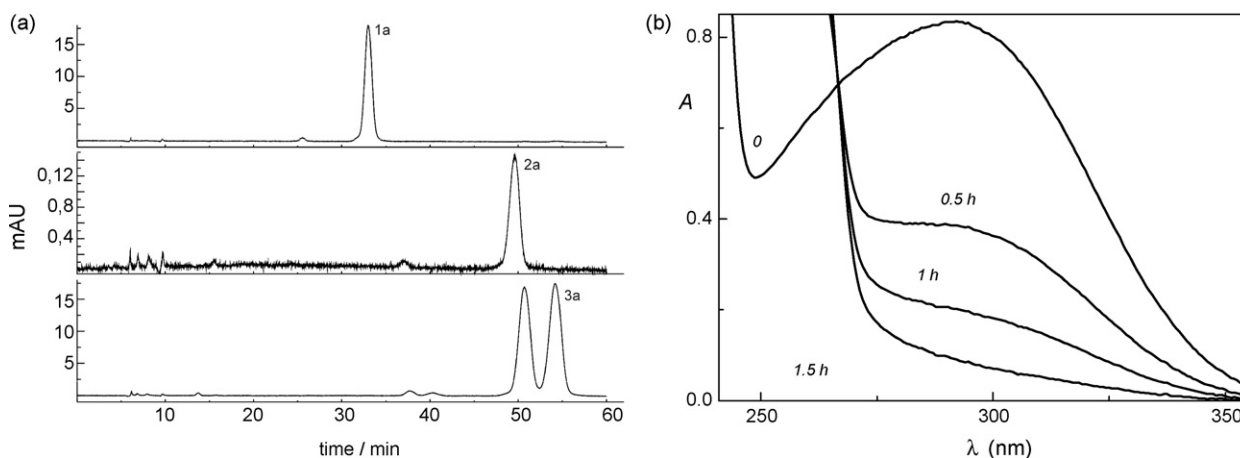


Fig. 2. HPLC traces for separation of **2a** and **3a** (a) and UV-absorption spectra prior to and during the irradiation of **1a** in acetonitrile (b).

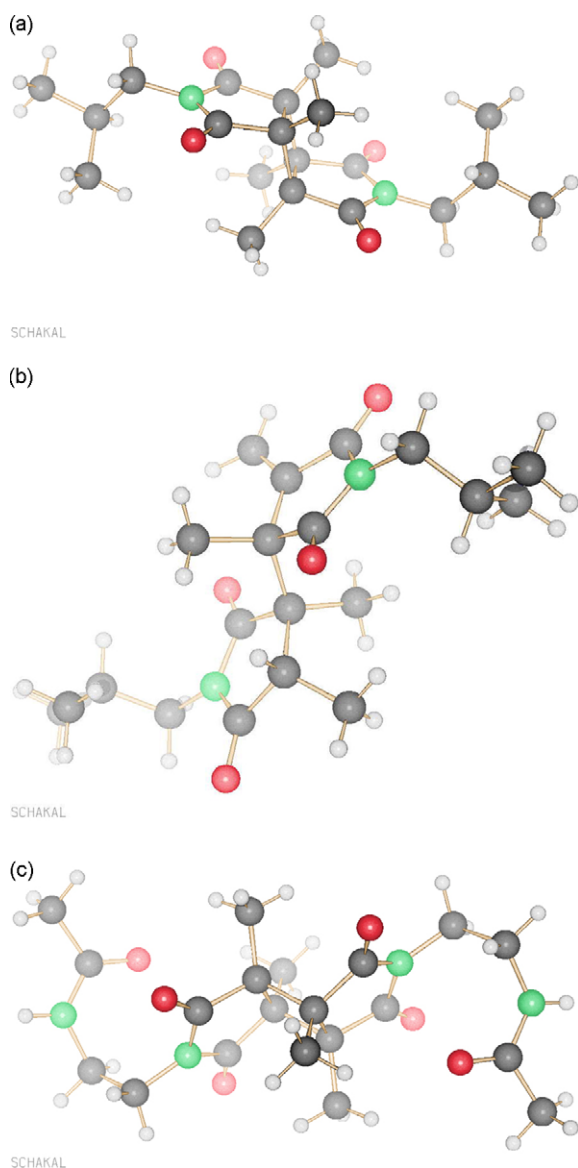


Fig. 3. X-ray structures of (a) **2a**, (b) **3a** and (c) **2b**.

in four solvents. These plots and data in Tables 1–3 reveal that the photochemical conversion initially increases linearly with irradiation time, approaching a maximum value. The slope of the initial part was taken as relative quantum yield of photodimerization. To account for changes in the lamp power, irradiation volume and DMI concentration, we used a second more specific measure for the photochemical conversion, pc^{rel} (Table 1) and a corresponding Φ_{dim}^{rel} (Table 4). Both relative quantum yields are normalized to the value of **1a** in argon-saturated cyclohexane. Absolute Φ_{dim} values for the photodimerization of DMI in various solvents using $\lambda_{irr} = 313$ nm are collected in Table 4. The absolute and relative values are consistent.

The results of product analyses after steady-state irradiation in the absence of sensitizers are collected in Table 1. Surprisingly high amounts (up to 50%) of **2a** were detected in various irradiated solutions of **1a**. Inspection of Table 1 reveals that under direct irradiation (i) the photodimerization of **1a** proceeds faster in solvents of low polarity (cyclohexane, 1,4-dioxane) than in solvents of higher polarity (methanol, acetonitrile), and that (ii) the fraction of **2a** (varying between 52 and 96%) decreases with increasing polarity of the solvent. As a measure of the polarity, we took the

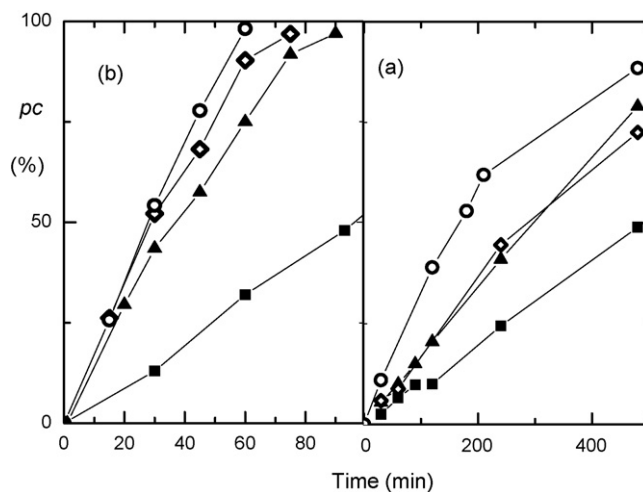


Fig. 4. Percentage of photochemical conversion pc (under argon) of **1a** into dimers vs. irradiation time; (a, conditions as in Table 1) in 1,4-dioxane (circles), dichloromethane (diamonds) acetone (triangles) and acetonitrile (squares), and (b) in the presence of $c(\mathbf{1a})$ (0.05 M) in methanol, $c(\text{thioxanthone})$: 0.5 (squares), 1 (diamonds) and 2 mM (circles), $c(\text{thioxanthone})/c(\mathbf{1b}) = 0.02$ (triangles), conditions as in Table 5.

Table 1

Photochemical conversion, pc, relative photochemical conversion and product ratios, **2:3**, at various irradiation times, t_{irr} , and concentrations, $c(\text{DMI})$, in solvents sorted by the polarity parameter

DMI	Solvent	E_{T}^{N}	$c(\text{DMI})$ (mM)	t_{irr} (min)	pc ^a (%)	pc ^{rel}	2:3		
1a	Cyclohexane	0.006	5	30	61	8.6	96:4		
			10	30	52	15	96:4		
			51	30	45 ^b	64.5	95:5		
			50	30	17	46			
				60	43	60	93:7		
			84	90	99 ^b		92:8		
				180	100 ^b				
			<i>n</i> -Hexane	0.009	50	120	86 ^b	30	93:7
			Benzene	0.11	51	480	50/68 ^b	12	84:16
			1,4-Dioxane ^c	0.16	52	480	89/96 ^b	17	94:6
	Ethyl bromide	0.22	50	90	65	9	77:23		
	Dichloromethane ^c	0.31	50	480	79 ^b	13	73:27		
	Acetone ^c	0.36	50	480	92.8 ^b	16	75:25		
	Acetonitrile ^c	0.46	50	480	49/64 ^b	12	64:36		
	Acetonitrile	0.46	48	40	54	16			
				60	76	15			
				120	93/99 ^b		62:38		
	Methanol	0.76	51	60	1.5	2			
				120	4	3			
				480	27.5 ^b	5	63:37		
Methanol- 1a			50	270	34	2	52:48		
			55	120	86	2	56:44		
Water (suspension)	1	50	480	64 ^b	11	80:20			
D ₂ O (suspension)	0.99	30	40	97	6	86:14			
Substance		– ^{c,d}	120	91 ^b		83:17			
1b	Cyclohexane (susp.)	0.006	5	240	5		98:2		
	Benzene	0.11	20	60	31 ^b	3	88:12		
	1,4-Dioxane	0.16	20	480	54 ^b	2	91:9		
	Acetonitrile	0.46	20	480	13/24 ^b	0.8	57:43		
			20	480	54	0.6	55:45		
	Methanol	0.76	20	480	11 ^b	0.4	80:20		
1c	Benzene	0.11	50	40	83.6	13	86:14		
	1,4-Dioxane	0.16	50	30	93	43	98:2		
	Acetonitrile	0.46	50	30	24	34			
				60	46	29			
				120	82	29	73:27		
	Acetonitrile		50	30	67/76 ^b	38	69:31		
	Acetonitrile ^{d,e}		50	30	44/52 ^b	26	75:25		
	Acetonitrile ^{d,e}		50	30	78	29			
				40	88	33	70:30		
	Methanol	0.76	50	30	13	6			
				120	55	8			
				180	86	7	57:43		
	Water	1	50	120	30	4			
			240	51	3	80:20			

^a In argon-saturated solutions at 25 °C, $\text{pc}^{\text{rel}} = \{\text{pc } v_{\text{irr}} c(\text{DMI}) / (I_p t_{\text{irr}})\} (10^3 \text{ mol/W s})$.

^b Values from NMR-spectra, otherwise from UV-spectra.

^c For shorter times see Fig. 4a.

^d 0.2 g (thin film).

^e Air-saturated.

frequently used parameter E_{T}^{N} [21]. A plot of the fraction of **2a** vs. E_{T}^{N} is shown in Fig. 5.

An apparent exception is the irradiation in water and in D₂O where the fraction of dimer **3** is lower than in the less polar methanol or acetonitrile. However, a suspension of **1a** in water was irradiated so that the ratio obtained might have been expected close to that in native solid form. In the case of **1b**, which is barely soluble in cyclohexane, we observe the highest pc in 1,4-dioxane and the highest product ratio **2b:3b** in 1,4-dioxane and cyclohexane, while in the protic solvents methanol and water the ratio increases compared to acetonitrile. For **1c** the ratio **2c:3c** decreases from 98:2 in 1,4-dioxane to ca. 70:30 in acetonitrile and to ca. 60:40 in methanol (following the order of increasing polarity) but increases in water to 80:20. Deviations in pc derived from UV and NMR spectra, respectively, result from general uncertainties in the integrals of small NMR-peaks on the one hand and from small contributions of **3** to the UV-absorption at 300 nm (Fig. 1), which are important at high

pc. The relative Φ_{dim} vs. E_{T}^{N} is shown in Fig. 5 for **1a**. Table 2 shows that in 1,4-dioxane the fraction of **2a** increases from 82 to 94% when the irradiation temperature was increased from 5 to 40 °C. This feature, however, does not pertain to acetonitrile solutions.

As expected the Φ_{dim} values increase with DMI concentration (Fig. 4, Table 1), approaching a maximum value. As, in principle, Φ_{dim} cannot exceed 0.5, the values observed for **1a** in cyclohexane and 1,4-dioxane, i.e. in low polarity solvents, are quite high. Φ_{dim} in ethyl bromide is somewhat large when compared to a solvent of similar polarity (Table 4). This might reflect a heavy atom effect supporting a triplet mechanism. The presence of oxygen decreases Φ_{dim} or pc^{rel} (Tables 1–4).

2.3. Sensitized photoconversion

The influence of sensitizers, such as thioxanthone, benzophenone, acetophenone or benzil, was studied in methanol and

Table 2
Effects of temperature on the photochemical conversion and product ratios of 0.05 M **1a**

T (°C)	t_{irr} (min)	pc (%) 1,4-Dioxane	2a:3a	pc (%) Acetonitrile	2a:3a
5 ^a	15			32	
	30	38/46 ^b	84:16	58	61:39
15	15	48		28	
	30	79/77 ^b	86:14	55	60:40
25	15	51		37	
	30	79/92 ^b	88:12	67	61:39
35	15	59		36	
	30	82/91 ^b	92:8	63	59:41
45	15	60		36	
	30	81/93 ^b	93:7	66	57:43

Upon irradiation in argon-saturated 1,4-dioxane and acetonitrile solutions of $v = 25 \text{ cm}^3$, lamp operated at 100 W, Duran glass filter.

^a Frozen solution in 1,4-dioxane.

^b Values derived from NMR-spectra, otherwise from UV-spectra.

Table 3
Effects of **1a** concentration on the photochemical conversion and product ratios

$c(\mathbf{1a})$ (M)	t_{irr} (min)	pc (%)	2a:3a
0.006	30	34	
	60	56	
	90	71	56:44
	120	79	
0.012	30	29	
	60	51	
	90	61	55:45
	120	66	
0.052	30	12	
	60	24	
	90	34	52:48
	120	45/97 ^a	
0.10	120	26/33 ^a	56:44
0.15 ^b	120	44/58 ^a	54:46

Upon irradiation in argon-saturated methanol at 25 °C, lamp at 90 W, Duran glass filter.

^a Values derived from NMR-spectra, otherwise from UV-spectra.

^b Precipitation during irradiation.

Table 4
Quantum yield of direct photodimerization^a

DMI	Solvent	E_T^N	$c(\text{DMI})$ (mM)	Φ_{dim}	$\Phi_{\text{dim}}^{\text{rel}}$
1a	Cyclohexane	0.006	6.6	0.047	1.0 ^b
			55	0.42	
			73	0.54	
	<i>n</i> -Hexane	0.009	5	0.034	0.09
			51	0.36	0.53
	Benzene	0.11	57	0.11	0.2
	1,4-Dioxane	0.16	13	0.18	(0.4) ^c
			50	0.24	0.3
	1,4-Dioxane ^d		6	0.006	
			55	0.06	
	Ethyl bromide	0.22	49	0.14	0.15
	Dichloromethane	0.31	1	0.010	(0.20)
			50	0.03	0.23
	Acetone	0.36	50		0.24
	Acetonitrile	0.46	5	0.01	(0.12)
			14	0.028	
51			0.098		
58			0.1		
Acetonitrile ^d		50	0.1		
		48	0.06		
		56	0.014	0.05	
Methanol	0.76	58	0.009		
Methanol- <i>d</i> ₁		50			
Water		50		0.04	
D ₂ O		30		0.2	
1b	Benzene	0.11	20	0.06	0.06
	1,4-Dioxane	0.16	20	0.07	0.03
			4	0.003	(0.14)
	Acetonitrile	0.46	12	0.011	
			24	0.055	0.01
			20		0.006
Methanol	0.76	20			
1c	Benzene	0.11	50	0.07	0.22
	1,4-Dioxane	0.16	50	0.38	0.75
	Acetonitrile	0.46	50	0.024	0.28
	Methanol	0.76	50		0.06

^a Φ_{dim} irradiated at 313 nm (Hatchard–Parker method) in argon-saturated solution at 25 °C.

^b Relative Φ_{dim} from $\text{pc}^{\text{rel}} = 1$ for **1a** in cyclohexane at 55 mM (mean value).

^c In parentheses: relative values from initial slopes in Fig. 4a irradiated through Duran filter.

^d Under air.

Table 5
Photosensitized conversion and product ratios of **1a** and **1b** in acetonitrile and methanol

DMI	Ip (W)	Solvent	Sensitizer	c(Sen) (mM)	c(Sen)/c(DMI)	t _{irr} (min)	pc (%)	2:3	
1a	30	Acetonitrile	None	0	–	30	11	61:39	
						60	23		
						30 ^b	43 ^b		
	30		Thioxanthone	1	0.02	60 ^b	75 ^b	53:47 ^b	
						5	18		
						10	36		
						15	53		
						20	75		
						30	94		
						40	98 ^a		
	15 ^b	100	59:41						
	30		Acetophenone	1	0.02	30	12	61:39	
						30 ^b	49 ^b	62:38	
	30		Benzophenone	1	0.02	30	23	60:40 ^b	
						30 ^b	75 ^b	61:39	
	30				10	0.2	30	74	60:40 ^b
							30 ^b	45	62:38
	30	Methanol	Thioxanthone	1	0.02	5	13	62:38	
						10	25		
						20	55		
30						85			
40						96			
5						74	50:50		
2						30			
8						92			
5						74			
30						5 ^a	62:38		
30		None	0	–	120	5 ^a	61:39		
					90 ^c	97 ^a	66:34		
					1	0.02	75 ^c	97 ^a	56:44
					2	0.04	60 ^c	98 ^a	66:34
100			1	0.02	2	44	62:38		
					5	99			
1b	30	Acetonitrile	None ^d	–	480	13	57:43		
		Methanol	Thioxanthone	1	0.07	30	100	62:38	
	30	Methanol	None ^d	1	0.05	480	11	80:20	
						60	100	79:21	

Upon irradiation through Duran glass filter in argon-saturated solutions of $v = 25 \text{ cm}^3$ at 25°C in the presence and absence of sensitizers at various concentrations ($c(\text{DMI}) = 0.015\text{--}0.05 \text{ M}$) and lamp powers (I_p).

^a Values derived from NMR-spectra, otherwise from UV-spectra.

^b Without Duran glass filter.

^c For shorter times see Fig. 4b.

^d From Table 1 at $c(\mathbf{1b}) = 0.02 \text{ M}$.

acetonitrile. Examples of plots of the photochemical conversion, pc, vs. irradiation time are shown in Fig. 4b for **1a** in methanol in the presence of thioxanthone. The results of irradiation of **1a** at various concentrations in argon-saturated methanol and acetonitrile are collected in Tables 5 and 6. For comparison, irradiation measure-

ments with acetophenone and benzophenone as sensitizers were also performed without the filter (Table 5).

Clearly, increasing concentrations of the sensitizer increases the photochemical conversion per time unit, while the product

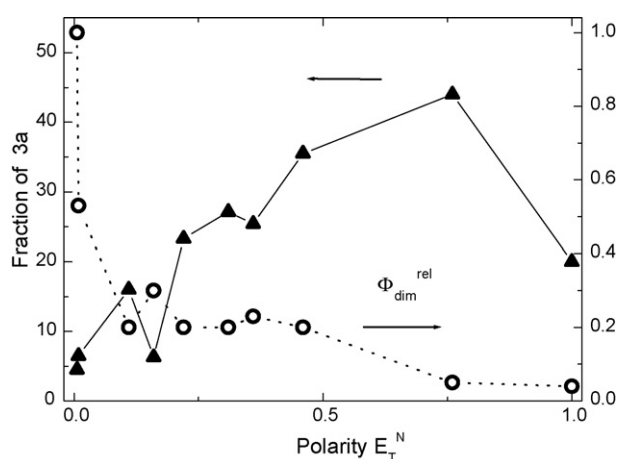


Fig. 5. Fraction of single-bonded dimer **3a** (\blacktriangle) and relative dimerization quantum yield (\circ) for **1a** as a function of solvent polarity, cf. Table 1.

Table 6

Photochemical conversion and product ratios upon irradiation of **1a** and **1b** in argon- and air-saturated methanol in the presence and absence of thioxanthone

DMI ^a	Gas	c(Sen) (M)	t _{irr} (min)	pc (%)	pc ^{rel}	2:3		
1a	Argon	0	30	12	5.6	52:48		
			60	24	5.6			
			90	34	5.3			
			120	45	5.2			
	Air	0	30	1.0	0.46	– ^b		
			90	4.4	0.68			
	Argon	0.001	10	10	98.7 ^a	137 ^a	58:42	
				Air	0.001	10		25.0
20						47.8		33
		30	65.1 ^a	30 ^a	53:47			
1b	Argon	0	480	10.5	0.4	80:20		
	Argon	0.001	60	100	>23	79:21		

Concentration of **1a**: 0.05 M, **1b**: 0.02 M; 25°C , $v_{\text{irr}} = 25 \text{ cm}^3$; lamp at 90 W, Duran glass filter.

^a Values derived from NMR-spectra, otherwise from UV-spectra.

^b Not sufficient product.

Table 7
Quantum yield of thioxanthone sensitized photodimerization^a

DMI	Solvent	c(thioxanthone) (mM)	c(DMI) (mM)	Φ_{dim}
1a	1,4-Dioxane	1	50	0.09
		0 ^b	50	0.24
	Acetonitrile	1	50	0.13
		0 ^b	50	0.1
1b	Acetonitrile	1	19	0.075
		0 ^b	12	0.011
		0 ^b	24	0.055

^a Argon-saturated at 25 °C, irradiated at 313 nm.

^b See Table 4.

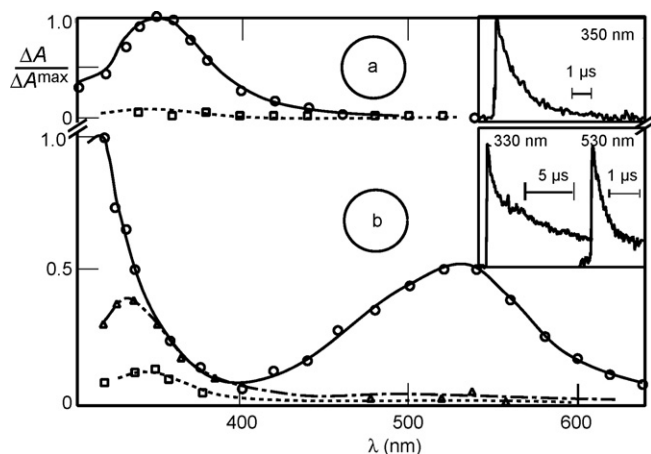


Fig. 6. Transient absorption spectra of (a) **1a** (1 mM) in argon-saturated cyclohexane and (b) benzophenone/**1a** in acetonitrile at 20 ns (○), 1 μs (Δ) and 10 μs (□) after the 308 nm pulse; insets: kinetics as indicated.

ratio **2a:3a** is hardly affected. In contrast the product ratio **2b:3b** in methanol shows large scatter (Tables 5 and 6, last two lines). The presence of thioxanthone does not enhance Φ_{dim} for **1a** in 1,4-dioxane (Table 7), because of the large Φ_{dim} value for direct irradiation, in contrast to the other solvents. The influence of oxygen was studied in methanol with thioxanthone as sensitizer (Table 6).

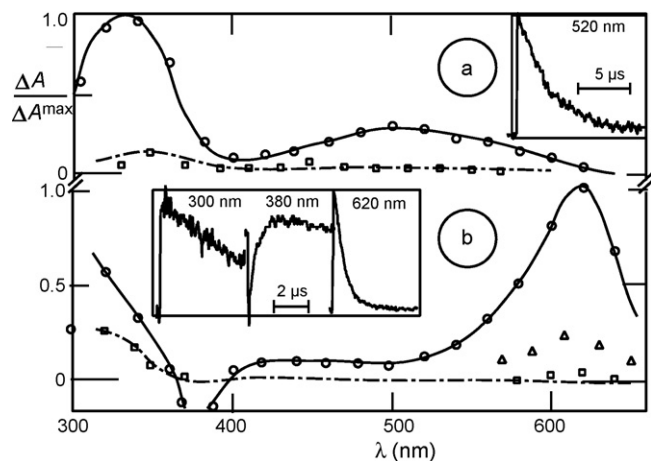


Fig. 7. Transient absorption spectra of (a) **1a** (1 mM) in argon-saturated benzene and (b) thioxanthone/**1a** in acetonitrile at 20 ns (○), 1 μs (Δ) and 10 μs (□) after the 308 nm pulse; insets: kinetics as indicated.

Table 8
Triplet parameters of *N*-alkylmaleimides and *N*-alkyl-Me₂-maleimides^a

M/DMI	Solvent	k_2 ($\times 10^9 \text{ M}^{-1} \text{ s}^{-1}$)	k_3 ($\times 10^7 \text{ M}^{-1} \text{ s}^{-1}$)
4a	Acetonitrile		190
4b	Acetonitrile	1.8	
4c	Acetonitrile		130 ^b
	Cyclohexane	2.2	3
	Benzene	1.3 (1) ^c	1 (1)
	1,4-Dioxane		<0.6
	Dichloromethane	1.3	0.5
1a	Acetonitrile	1.8 (1.6)	1.2 (1)
	Methanol	1.5 (1.4)	0.8 (1)
	Benzene	1.0	

^a For DMI k_2 under argon and $\lambda_{\text{exc}} = 308 \text{ nm}$.

^b From Ref. [19].

^c Values in parentheses refer to **1b**.

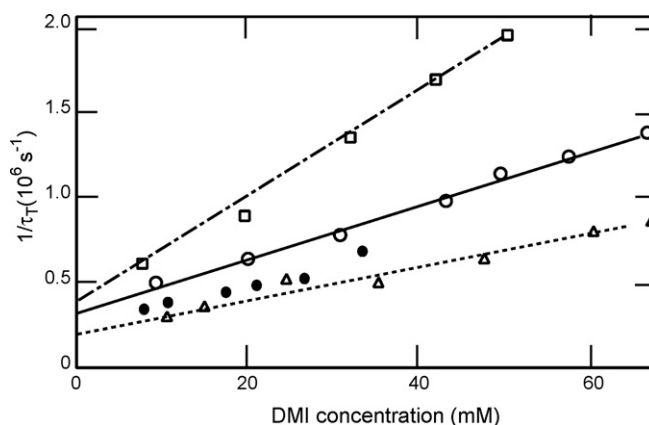


Fig. 8. Plots of $1/\tau_T$ vs. the concentration for **1a** (open) and **1c** (full) in argon-saturated cyclohexane (squares), benzene (triangles) and acetonitrile (circles).

2.4. Triplet properties

A transient absorbing at 300–400 nm is formed at the end of the pulse upon 308 nm excitation of **1a** in cyclohexane and **1a–c** solvents of larger polarity. Transient absorption spectra are presented in Figs. 6 and 7. The maximum is generally at $\lambda_T = 350 \text{ nm}$ and only for **1a–c** in benzene a weak band appears also in the 400–600 nm range. The transient is assigned to the lowest triplet state, generated by intersystem crossing. The triplet state is quenched by oxygen and the triplet lifetime (τ_T) of **1a–c** (at <1 mM) in argon-saturated solution is 2–20 μs. The triplet decay follows first-order kinetics at low pulse intensities (e.g. <1 MW cm⁻²) and can be fitted by an additional second-order component due to T–T annihilation, when the intensity is higher. The rate constant for quenching of **1a** by oxygen in cyclohexane or acetonitrile is $k_2 = (1.8\text{--}2.1) \times 10^9 \text{ M}^{-1} \text{ s}^{-1}$ (k_i refer to steps of the reaction mechanism, see below) and the values in other cases are only slightly smaller (Table 8). The inverse lifetime $1/\tau_T$ increases with increasing DMI concentration. Examples are shown in Fig. 8. The rate constant for this so-called self-quenching was estimated to be $k_3 = 1 \times 10^7 \text{ M}^{-1} \text{ s}^{-1}$.

The observed results for *N*-alkyldimethylmaleimides are intersystem crossing (1), quenching of the triplet state by oxygen (2) and self-quenching (3). Those for *N*-alkyl-maleimides (M) have been treated accordingly [19,20].



Table 9
Quantum yields of singlet molecular oxygen formation, Φ_{Δ} , and dimerization, Φ_{dim} , for DMI^a

Solvent	Φ_{Δ}			Φ_{dim}^b		
	1a	1b	1c	1a	1b	1c
Cyclohexane	0.46			0.4		
Benzene	0.40	0.15	0.42	0.1	0.04	0.1
1,4-Dioxane	0.22	0.08 (0.08) ^c	0.28	0.2	0.03	0.35
Dichloromethane	0.14	0.08	0.16	0.1		
Acetonitrile	0.10	0.03 (0.04)	0.12	0.1	<0.03	0.14
Methanol				0.02		0.03

^a Under argon at 25 °C, $\lambda_{\text{exc}} = 308$ nm.

^b Averages, see Table 4.

^c Values in parentheses refer to **1d**.

Singlet molecular oxygen, $\text{O}_2(^1\Delta_g)$, may be expected from reaction (2) and was indeed detected for DMI (Table 9). The self-quenching occurs in a complex ($^3\text{DMI} \cdots \text{DMI}$) which may react – via a biradical or zwitterionic intermediate, respectively (cf. Scheme 3) – into the two dimers **2** and **3** or back into the unchanged monomers. The solvent polarity has only little effect on the kinetic parameters of the steps 2 and 3 but affects the product distribution (see above). We could also detect the triplet state of the polymer **1d** in either 1,4-dioxane or acetonitrile.

Singlet oxygen is formed in reaction (2) (along with minor oxygen species) [22]. The quantum yield of the emission of singlet oxygen, Φ_{Δ} , is a minimum for the intersystem crossing quantum yield, Φ_{isc} . The Φ_{Δ} values show the same trend as Φ_{dim} i.e. they are lower for **1b** than **1a** or **1c** and decrease with increasing solvent polarity (Table 9).

The reaction under sensitized conditions is initiated by excitation of the energy donor (S), followed by intersystem crossing and energy transfer (4) from the ^3S triplet.



The donor triplet state in argon-saturated acetonitrile, which is formed within the 308 nm pulse, displays the well-known absorption spectrum with maxima at 320 and 520 nm for benzophenone and at 620 nm for thioxanthone, respectively [23].

On addition of **1a**, the decay of the triplet state of the donor is faster than in their absence, but no new transient absorption was detected above 400 nm. A longer-lived transient absorption at $\lambda_T = 350$ nm is observable (Figs. 6b and 7b). This second transient is ascribed to the acceptor triplet state, ^3DMI . The rate constant for quenching of the benzophenone triplet state by **1a**, **1b** and **1c** was estimated to be $k_4 = 12 \times 10^9$, 10×10^9 and $9 \times 10^9 \text{ M}^{-1} \text{ s}^{-1}$, respectively. The results for thioxanthone are analogous. Decay of ^3S and formation of ^3DMI are expected to show the same kinetics, but the grow-in of the acceptor triplet state absorption is mostly overlapped by that of the donor.

3. Discussion

3.1. Photodimerization

Since the formation of single-bonded dimers analogous to **2b** and **3b** was not reported in **4a–d** [10–20], it can be concluded that the presence of the DMI methyl groups is a necessary prerequisite for the occurrence of the single-bonded dimer. This shall be discussed on the basis of Scheme 3. When product distributions and quantum yields are compared (see Fig. 5, Tables 1, 3 and 4) it is obvious that dimerization quantum yields diminish with increasing polarity of the solvent while the fraction of **3a** rises. This suggests an increase of both, bipolar (zwitterionic) character of the intermediate and its torsion (due to solvation) with solvent

polarity. The distorted bipolar intermediate mainly stabilises via re-dissociation into **1a** but to some extent a proton migration takes place to form **3a** (Scheme 3, cf. Eq. (3')) via intramolecular deprotonation of the $^+\text{C}-\text{CH}_3$ part into a $\text{C}=\text{CH}_2$ part and protonation of the $^-\text{C}-\text{CH}_3$ into $\text{HC}-\text{CH}_3$. Two exceptions from the trend that Φ_{dim} decreases with solvent polarity (as revealed by E_T^N -values) are benzene, where Φ_{dim} is only 0.04–0.1, and ethyl bromide, where Φ_{dim} is comparatively large (Fig. 5) and a heavy atom effect (increasing Φ_{isc}) might be involved. Both the exceptions can be caused by specific solvation effects of the two solvents, which are not accounted for in the E_T^N scale.

Both the influence of the sensitizer and the sensitivity of the photochemical conversion against oxygen are strong indications of a triplet mechanism in the photodimerization. Oxygen quenching is more prominent at low DMI concentrations, since at higher concentration self-quenching competes, which leads to dimers. The finding that there is no obvious dependence of the product ratio on monomer concentration indicates no obvious state selectivity (Tables 1 and 4–6). A small temperature dependence was found for the ratio **2a:3a** (Table 2). At higher irradiation dose the ratio decreases from 61:39 to 1:1 (Table 5, lines 2 vs. 4).

3.2. Triplet reactions of *N*-alkylmaleimides

The end of pulse transient of *N*-alkylmaleimides (M) has been assigned to the lowest triplet state [16,18,10]. For **4b**, **4c** and **4d** $\Phi_{\text{isc}} = 0.03$, 0.07 and 0.24, respectively [11,17]. For **4b** in acetonitrile and water $k_2 = 1.8 \times 10^9 \text{ M}^{-1} \text{ s}^{-1}$ [17,20]. The ^3M state is the proposed precursor of the photodimers; data for M are compiled in Table 8. The kinetics of triplet decay are affected by the M concentration, unless the ground state involves a complex other than from the photodimers. The complex ($^3\text{M} \cdots \text{M}$) may react into cyclobutane fused dimers (M_2) or back into the unchanged monomers with probabilities β and $1 - \beta$, respectively. A single-bonded dimer corresponding to **3** has not been reported.



The rate constant for self-quenching of *N*-alkylmaleimides is close to the diffusion-controlled limit and plays therefore a decisive role. For **4a** (<1 mM) in argon-saturated aqueous solution $\tau_T = 5 \mu\text{s}$ and $k_3 = 2.6 \times 10^9 \text{ M}^{-1} \text{ s}^{-1}$, the latter also in acetonitrile [18,19]. The triplet lifetime of **4b** (<2 mM) in argon-saturated acetonitrile is $\tau_T = 0.16$ – $0.17 \mu\text{s}$ and $k_3 = 1.9 \times 10^9 \text{ M}^{-1} \text{ s}^{-1}$ and $\tau_T = 0.77 \mu\text{s}$ and $k_3 = 1.6 \times 10^9 \text{ M}^{-1} \text{ s}^{-1}$ in water [12,20]. For **4c** in carbon tetrachloride or acetonitrile $k_3 = 1.8 \times 10^9$ and $6 \times 10^8 \text{ M}^{-1} \text{ s}^{-1}$ in water [19]. For *N*-butylmaleimide, **4d**, in deoxygenated dichloromethane the quantum yield of dimerization using $\lambda_{\text{irr}} = 310$ nm is $\Phi_{\text{dim}} = 0.06$, that of disappearance of **4d** is 0.12 [11].

The results for sensitized photolysis in an inert solvent reveal a larger Φ_{dim} . A literature value for benzophenone and **4b** in acetonitrile is $k_4 = 7.8 \times 10^9 \text{ M}^{-1} \text{ s}^{-1}$ [12]. In non-inert solvents (DH) H-atom transfer to the $^3(n,\pi^*)$ triplet state of a ketone or diketone is a common photoreaction which follows the general equation



The radicals MH^\bullet and D^\bullet undergo several termination reactions. For quenching by ethanol or 2-propanol a rate constant of $k_5 < 1 \times 10^6 \text{ M}^{-1} \text{ s}^{-1}$ was found. For triplet quenching of **4a** in acetonitrile by 2-propanol and ethanol, $k_5 = 5.7 \times 10^7$ and $1.5 \times 10^7 \text{ M}^{-1} \text{ s}^{-1}$, respectively and the values in water are 18×10^7 and $3 \times 10^7 \text{ M}^{-1} \text{ s}^{-1}$ [19]. As a comparison, for **4a** and **4b** (<1 mM) in argon-saturated acetonitrile $k_5 = (1-6) \times 10^7 \text{ M}^{-1} \text{ s}^{-1}$ [19]. On addition of an electron donor D radical ions are formed via general

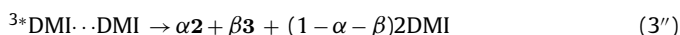
equation



Literature values for k_6 are $(1-9) \times 10^9 \text{ M}^{-1} \text{ s}^{-1}$ for **4a** in acetonitrile or water and several electron donors, such as 2,3- or 2,5-dihydrofuran and several vinyl ethers [19,20].

3.3. Triplet properties of *N*-alkyl-3,4-dimethylmaleimide

For **1a–c** our results are in agreement with steps (1)–(4). However, a branching of the dimerization reaction into **2** and **3** affords a modification of Eq. (3): (${}^3\text{DMI} \cdots \text{DMI}$) may react into the assumed biradical or bipolar intermediate (Scheme 3) and then either into dimers (**2,3**) or back into the unchanged monomers with probabilities α, β and $1 - \alpha - \beta$, respectively; $(\alpha + \beta) \leq 1$.



Processes according to (5) and (6) were not detected or minor. This is a consequence of 4,5-dimethyl substitution. The transient of **1a–c** formed concomitant to the pulse is assigned to the lowest triplet state. This is confirmed by energy transfer. The rate k_4 constant for quenching of triplet benzophenone by **1a–c** in acetonitrile is diffusion controlled. Striking differences were found for the two *N*-alkyl-3,4-dimethylmaleimides with respect to *N*-alkylmaleimides: low reactivity towards H-atom abstraction and quenching by the DMI ground state. The former effect allows methanol or other alcohols as medium for direct irradiation, in contrast to *N*-alkylmaleimides and ketones. The lower k_5 values allow the observation of the triplet decay in a more appropriate concentration range. On the other hand, the low ϵ_{300} of the **1a** monomer allows irradiation of a 0.01–0.1 M concentration and thus conditions of >50% self-quenching.

When the DMI concentration becomes larger, e.g. 0.05 M, triplet quenching by oxygen is less efficient. This is reflected by $\Phi_{\text{dim}} = 0.06$ vs. 0.24 for **1a** in 1,4-dioxane in the presence vs. absence of air, respectively (Table 4). It can, however, not account for the similarity (0.1) for **1a** in air- and argon-saturated acetonitrile.

3.4. Does photodimerization occur bypassing the triplet route?

As mentioned above (see Section 3.1) our experimental data point to a triplet mechanism in the photodimerization throughout. A **1a** concentration of 6 mM (Table 6) is sufficient for dimerization. This is roughly in line with the estimate of $1/\tau_T \times k_3 = 10 \text{ mM}$, taking $k_3 = 1 \times 10^7 \text{ M}^{-1} \text{ s}^{-1}$ and $\tau_T = 10 \mu\text{s}$.

With a few exceptions Φ_{dim} for **1a**, **1b** and **1c** is relatively low, depending on solvent and concentration. The latter follows Eq. (7), if the triplet route is operating [11].

$$\Phi_{\text{dim}} = \Phi_{\text{isc}} \cdot k_3 c(\text{DMI}) / (k_2 + k_3 c(\text{DMI})) \quad (7)$$

Φ_{dim} thus cannot exceed the triplet quantum yield, which corresponds to Φ_{Δ} and amounts to 0.02–0.4; these values account for the changes in Φ_{dim} (Table 9). Therefore, dimerization from the singlet state needs not be discussed.

3.5. Polymers

The previous discourse in the literature as to whether or not a sensitizer is necessary to form crosslinks in polymers can be supplemented on the basis of our work: dimerization is possible without sensitizer as DMI moieties at high loading in the polymer are close enough for efficient self-quenching of the triplet state; at lower loading a sensitizer increases the yield and therefore decreases the irradiation time. Moreover, photochemical side reactions of the

polymer backbone are remote in the sensitized reaction, since a wavelength can be used which is not absorbed by the polymer backbone.

4. Conclusions

Two types of dimers, the usual cyclobutane-type cyclic dimer (**2**) and one with a single-bound structure (**3**), were observed for three *N*-alkyl-3,4-dimethylmaleimides, **1a–c** under all conditions. They are probably formed from a common so far undetected single-bonded intermediate, which exists in biradical or bipolar forms. The product ratio **2:3** can be steered between ca. 9:1 and 1:1 by choosing solvents of different polarity. The ratio depends, to a lower extent, also on the reaction temperature and irradiation wavelength. The detection of the single-bonded dimer **3** does not diminish the suitability of DMI derivatives for crosslink formation in polymers. The quantum yield of dimerization under direct irradiation is generally low or moderate, but can be quite high for **1a** and **1c** in certain solvents of low polarity. The photodimerization of the dimethylmaleimides is suggested to proceed through the triplet state, whose lifetime is quite long when compared to maleimides, whereas the rate constant for triplet self-quenching is less efficient. A singlet mechanism for dimerization, e.g. at high concentrations, is not proposed. The presence of sensitizers, such as benzophenone or thioxanthone, enhances the dimerization efficiency.

5. Experimental

5.1. Chemicals

Solvents used for pulsed and steady-state irradiation measurements were spectroscopic grade (or better), solvents used for the preparation of **1a** and **1b** were at least p.a. quality. Butylamine and toluene were purified by distillation over KOH. *N*-Isopropyl acrylamide (97% Acros) was recrystallized from *n*-hexane and dried in vacuum. Dimethyl maleic anhydride (97% Lancaster), *N*-acetyl diamine (98% Sigma–Aldrich), β -alanine (99% Merck) were used as received. The sensitizers obtained from Sigma–Aldrich were >99%.

5.2. Spectra

The ${}^1\text{H}$ NMR and ${}^{13}\text{C}$ NMR spectra were recorded on a Bruker DRX 500 spectrometer (500 MHz). UV–vis spectra were measured on Lambda 35 (PerkinElmer) spectrometer. For FT-IR a Nicolet 5700 (Thermo Elektron Dreieich) was used.

Element analyses were carried out on a Hekatech EA 3000 Euro Vector CHNSO Elementaranalysator. Melting points were determined on a Büchi-B 545. Molecular weight and molecular weight distribution were obtained by size exclusion chromatography using a PL-120 equipped with two GRAM columns (GRAM 103 Å and GRAM 102 Å PSS) and RI detector. The measurements were carried out in *N,N*-dimethylacetamide with 0.42 wt% LiBr at 50 °C with a flow rate of 1.0 mL/min. PMMA standards were used for calibration.

5.3. Substances

N-Isobutyl-3,4-dimethylmaleimide (**1a**, 1-isobutyl-3,4-dimethyl-1*H*-pyrrole-2,5-dione). 14.1 g (0.19 mol) of butylamine was added to a stirred solution of 5 g (0.04 mol) dimethylmaleic anhydride in 250 mL of toluene. The mixture was refluxed at 130 °C using a water separator. The solvent was evaporated under reduced pressure. Minor products were removed by filtration through silica gel using ethylacetate as solvent. The product was purified via column chromatography. (*n*-hexane:ethylacetate, 4:1) to yield 4.5 g,

0.025 mol (62.5%) of a colorless liquid. ^1H NMR (500 MHz, CDCl_3 , δ in ppm): 3.14 (2H, CH_2), 1.84 (6H, $\text{CH}(\text{CH}_3)_2$), 1H, $\text{CH}(\text{CH}_3)_2$), 0.75 (6H, CH_3). ^{13}C NMR (CDCl_3 , 500 MHz, δ in ppm): 8.4 (2 CH_3), 19.7 (2 CHCH_3), 27.6 (CH), 45.0 (N– CH_2), 136.6 (C=C), 172.1 (2 C=O). IR ($\tilde{\nu}$ cm^{-1}): 2962 (C–H), 1713 (C=O), 1621 (C=C), 1408 (C–H). Elemental analysis: $\text{C}_{10}\text{H}_{15}\text{NO}_2$, calc. C: 66.27%, H: 8.34%, N: 7.73%; exp. C: 66.22%, H: 8.36%, N: 7.81%.

N-(2-Acetamido)ethyl-3,4-dimethylmaleimide (**1b**, *N*-[2-(3,4-dimethyl-2,5-dioxo-2,5-dihydro-1H-pyrrol-1-yl)ethyl]acetamide).

19.5 g (0.19 mol) of *N*-acetyl ethylene diamine was added to a stirred solution of 5 g (0.04 mol) dimethylmaleic anhydride in 250 mL of toluene. The mixture was refluxed at 130 °C using a water separator. The solvent was evaporated under reduced pressure. The resulting waxy mass was dissolved in 100 mL chloroform, extracted twice with 50 mL water and with 50 mL of brine. After drying over NaSO_4 the solution was concentrated. The resulting white crystals were achieved by precipitating into cold *n*-pentane and dried in vacuo. Yield 6.5 g (77%). ^1H NMR (CDCl_3 , 500 MHz, δ in ppm): 7.25 (s, 1H, NH); 3.65 (m, 2H, N– CH_2), 3.42 (m, 2H, NH– CH_2), 1.96 (s, 6H, CH_3), 1.93 (s, 2H, CH_3). ^{13}C NMR (CDCl_3 , 500 MHz, δ in ppm): 172.6 (2 C=O), 170.5 (NH–C=O), 137.9 (C=C), 40.5 (NH– CH_2), 37.6 (N– CH_2), 8.6 (2 CH_3). IR (KBr): ($\tilde{\nu}$ cm^{-1}): = 2934 (C–H), 1713 (C=O), 1657 (amide I), 1625 (C=C), 1546 (amide II). Elemental analysis: $\text{C}_{10}\text{H}_{14}\text{N}_2\text{O}_4$, calc. C: 57.13%, H: 6.71%, N: 13.33%; exp. C: 57.12%, H: 6.75%, N: 13.3%.

N-(3-Propionic acid)-3,4-dimethylmaleimide (**1c**, *N*-[2-(3,4-dimethyl-2,5-dioxo-2,5-dihydro-1H-pyrrol-1-yl)-ethyl]-carboxylic acid) was prepared as described in the literature [24] and showed the physical and spectroscopic properties published there.

The polymer **1d** was available from previous investigations [8]. The polymer contained 5% (w/w) of **1b**. **4a**, **4b** were purchased from Ega and used as supplied.

5.4. Physical and spectral data of reaction products

(*N,N*-Diisobutyl)-1,2,3,4-tetraacetyl-diimido-cyclobutane (**2a**) (Scheme 3). Colorless rhombic crystals, mp 202 °C. UV $\lambda_{\text{max}} = 254.6$ nm (MeOH). ^1H NMR (500 MHz, CDCl_3 , δ in ppm): 3.37 (4H, d, $J = 7.3$ Hz), 2.07 (2H, m), 1.17 (6H, s), 0.92 (6H, d, $J = 7.7$ Hz). ^{13}C NMR (500 MHz, CDCl_3 , δ in ppm): 177.9 (q, C=O), 49.5 (q), 46.6 (d, CH_2), 27.1 (t, CH), 20.3 (s, CH_3), 13.3 (s, CH_3). ESI-MS: 363.2 $[\text{M}+\text{H}]^+$, 380.2 $[\text{M}+\text{NH}_4]^+$. Element analysis: $\text{C}_{20}\text{H}_{30}\text{N}_2\text{O}_4$, calc. C: 66.27%, H: 8.34%, N: 7.73%; exp. C: 66.57%, H: 8.77%, N: 7.60%.

2b. mp 273 °C. ^1H NMR (500 MHz, CDCl_3 , δ in ppm): 5.74 (2H, m, NH), 3.71 (4H, m, CH_2), 3.52 (4H, m, CH_2), 1.89 (6H, s, COCH_3), 1.16 (12H, s, CH_3). ^{13}C NMR (500 MHz, CDCl_3 , δ in ppm): 178.1 (q, C=O), 170.8 (q, C=O), 49.7 (q, C), 39.2 (d, CH_2), 38.3 (d, CH_2), 23.2 (t, CH), 12.7 (s, CH_3). ESI-MS: 421.2 $[\text{M}+\text{H}]^+$.

2c. mp 299–301 °C. ^1H NMR (500 MHz, $\text{DMSO}-d_6$, δ in ppm): 12.49 (2H, s, COOH), 3.68 (4H, t, CH_2), 2.62 (4H, t, CH_2), 1.05 (12H, s, CH_3).

3a (Schemes 3 and 4) was isolated from the irradiated mixture via high performance liquid chromatography (HPLC Knauer): at 23 °C, column diameter 8 mm, length 300 mm, stationary phase Eurospher-100, eluent MeOH:H₂O = 70:30, volume flow 1 cm³/min, UV-Detector 254 nm; fraction at 53–58 min retention time, see Fig. 2a. After multiple HPLC runs sufficient material was collected for NMR and X-ray studies. Mp 126–127 °C. UV: $\lambda_{\text{max}} = 241$ nm (in CDCl_3). ^1H NMR (500 MHz, CDCl_3 , ppm): 6.50 (s, H-18a), 5.94 (H-18b), 3.40 (m, H-13), 3.27 (d, $J = 7.29$ Hz, H-4), 3.17 (q, $J = 7.16$ Hz), 2.06 (m, H-14), 2.01 (m, H-5), 1.45 (s, H-11), 1.26 (s, H-8), 1.20 (d, $J = 7.35$ Hz, H-2), 0.91 (d, $J = 5.18$, H-15), 0.90 (d, $J = 5.16$, H-15), 0.86 (d, $J = 6.97$ Hz, H-6), 0.84 (d, $J = 6.89$ Hz, H-6). ^{13}C NMR (500 MHz, CDCl_3 , δ in ppm): 179.7 (q, C=O, C-7), 178.8 (q, C=O, C-3), 177.8 (q,

C=O, C-12), 168.8 (q, C=O, C-16), 140.5 (q, C=, C-17), 123.2 (d, $\text{CH}_2=$, C-18), 50.4 (q, C-9), 49.3 (q, C-10), 46.4 (d, C-13), 46.1 (d, C-4), 40.7 (t, C-1), 27.3 (t, C-14), 27.0 (t, C-5), 20.7 (s, C-15), 20.2 (s, C-15), 20.0 (s, C-6), 20.0 (s, C-6), 19.6 (s, C-11), 16.8 (s, C-8), 11.9 (s, C-2). ESI-MS: 363.2 $[\text{M}+\text{H}]^+$, 380.2 $[\text{M}+\text{NH}_4]^+$.

3b and **3c** were identified in reaction mixtures by prominent NMR-signals analogous to **3a**.

For X-ray analyses of **2a**, **3a** and **2b** see Supporting material. Data have been deposited with the Cambridge Crystallographic Data Centre as supplementary publications no. CCDC-669814-669816.

5.5. Continuous irradiation

Stirred argon-saturated solutions (typically 25 cm³) thermostatted at 25 °C were irradiated through the gas–liquid interface using a 200 W Xe-Hg lamp (AMKO). In most experiments the light was filtered through Duran glass, i.e. wavelengths > 300 nm reached the samples. Solvents were spectroscopic grade. Photochemical conversions, pc, were determined after irradiation and appropriate dilution (re-dissolving possible precipitates) via UV-spectroscopy. Alternative pc values were derived from NMR-spectra of irradiated samples, which were taken after evaporation of the solvent and dissolving the residue in NMR-solvents (CDCl_3 , $\text{DMSO}-d_6$, D_2O). Quantum yields of photodimerization were measured using the Hatchard–Parker method [25]. For this purpose argon-purged DMI solutions (0.005 and 0.5 M) were irradiated at room temperature in 1 cm × 1 cm cuvettes so that total absorption of the light was ensured. For DMI solutions at lower concentrations cuvettes with longer path lengths were used. Quantum yields Φ_{dim} were reproducible within ±10%. Relative quantum yields were calculated either from initial slopes of pc vs. time plots ($\Phi_{\text{dim}}^{\text{rel}}$) or from pc values corrected by irradiated volume, lamp power, irradiation time and DMI concentration ($\Phi_{\text{dim}}^{\text{rel}}$). Ratios of the two dimeric products were determined from selected peaks of the dimers a and b in the NMR spectra, see Supporting material. Values for the ratios of the two dimers are reproducible within ±3%. Neither Φ_{dim} nor product ratios are significantly affected by the irradiation wavelength, i.e. irradiation through Duran glass, through quartz glass ($\Phi_{\text{Duran}}/\Phi_{\text{none}} = 0.36$) or through a monochromator at 313 nm (for Φ_{dim} determinations) lead to consistent results. In benzil-sensitized reactions the Duran glass filter had to be removed in order for the sensitizer to absorb light.

5.6. Flash photolysis

For photolysis with UV–vis detection an excimer laser with 248 or 308 nm excitation (rise time <20 ns), a transient digitizer (Tektronix 7912AD) and an Archimedes 440 computer for data handling were used as in previous work [2i]. As the results turned out to be similar for $\lambda_{\text{exc}} = 248$ or 308 nm, only the latter was applied, which made possible to excite in benzene, for example. Formation of singlet molecular oxygen, $\text{O}_2(^1\Delta_g)$, was detected by a Ge-diode. The emission signal at 1260 nm is maximum within 1 μs and decays within a lifetime of 30–100 μs , depending on the solvent [22a]. It was ascertained that the emission can be fully suppressed by purging with argon. The quantum yield (Φ_{Δ}) in air-saturated solution was obtained from the slope of the maximum as a function of the laser intensity using optically matched solutions and phenazine in dichloromethane ($\Phi_{\Delta} = 0.89$) as Ref. [26].

Acknowledgements

Thanks are due to Anne Jäger for the X-ray investigations, Professor Wolfgang Lubitz for his support, and Mr. Horst Selbach, Leslie J.

Currell and Andrea Göpfert for technical assistance. Financial support by the Deutsche Forschungsgemeinschaft (SFB 287, TP A13, TP B10) is gratefully acknowledged.

Appendix A. Supplementary data

Supplementary data associated with this article can be found, in the online version, at doi:10.1016/j.jphotochem.2008.02.013.

References

- [1] (a) J. Fritsche, *J. Prakt. Chemistry* 102 (1867) 333;
(b) H. Bouas-Laurant, A. Castellan, J.P. Desvergne, R. Lapouyade, *Chem. Soc. Rev.* 30 (2001) 248–263;
(c) A. Schütz, T. Wolff, *J. Photochem. Photobiol. A: Chem.* 109 (1997) 251–258;
(d) C. Lehnberger, D. Scheller, T. Wolff, *Heterocycles* 45 (1997) 2003–2039.
- [2] (a) G. Ciamician, P. Silber, *Ber. Dtsch. Chem. Ges.* 35 (1902) 4128–4131;
(b) F.D. Lewis, *Adv. Photochem.* 13 (1986) 165–235;
(c) T. Wolff, F. Schmidt, P. Volz, *J. Org. Chem.* 57 (1992) 4255–4262;
(d) G.S. Hammond, C.A. Stout, A.A. Lamola, *J. Am. Chem. Soc.* 86 (1964) 1306–3103;
(e) C.H. Krauch, S. Farid, G.O. Schenck, *Chem. Ber.* 99 (1966) 625;
(f) R. Hoffmann, P. Wells, H. Morrison, *J. Org. Chem.* 36 (1971) 102–108;
(g) F.D. Lewis, D.K. Howard, J.D. Oxman, *J. Am. Chem. Soc.* 105 (1983) 3344–3345;
(h) X. Yu, D. Scheller, O. Rademacher, T. Wolff, *J. Org. Chem.* 68 (2003) 7386–7399;
(i) T. Wolff, H. Görner, *Chem. Phys. Phys. Chem.* 6 (2004) 368–376.
- [3] (a) I. von Wilucki, H. Matthäus, C.H. Krauch, *Photochem. Photobiol.* 6 (1967) 497–500;
(b) A.A. Lamola, T. Yamane, *Proc. Natl. Acad. Sci. U.S.A.* 58 (1967) 443–446.
- [4] (a) X. Coqueret, *Macromol. Chem. Phys.* 200 (1999) 1567–1579;
(b) N. Kawatsuki, K. Goto, T. Yamamoto, *Liq. Cryst.* 28 (2001) 1171–1176;
(c) R. Schinner, T. Wolff, *Colloid Polym. Sci.* 279 (2001) 1225–1230.
- [5] (a) H. Zweifel, *Photogr. Sci. Eng.* 27 (1983) 114–118;
(b) J. Berger, H. Zweifel, *Angew. Makromol. Chem.* 115 (1983) 163–179;
(c) J. Finter, E. Witmer, H. Zweifel, *Angew. Makromol. Chem.* 128 (1984) 71–97;
(d) J. Finter, Z. Haniotis, F. Lohse, K. Meier, H. Zweifel, *Angew. Makromol. Chem.* 133 (1985) 147–170.
- [6] M. Roth, B. Müller, *Polym. Paint Color* 178 (1988) 209–212.
- [7] (a) F.C. De Schryver, N. Boens, G. Smets, *J. Polym. Sci. A* 10 (1972) 1687–1697;
(b) F.C. De Schryver, N. Boens, G. Smets, *Macromolecules* 7 (1974) 399–406;
(c) F.C. De Schryver, N. Boens, G. Smets, *J. Am. Chem. Soc.* 96 (1974) 6463–6469.
- [8] (a) D. Kuckling, M. Harmon, C. Frank, *Macromolecules* 35 (2002) 6377–6383;
(b) D. Kuckling, J. Hoffmann, M. Plötner, D. Ferse, K. Kretschmer, H.-J.P. Adler, K.-F. Arndt, R. Reichelt, *Polymer* 44 (2003) 4455–5562;
(c) M.E. Harmon, D. Kuckling, P. Pareek, C.W. Frank, *Langmuir* 19 (2003) 10947–10956;
(d) D. Kuckling, C.D. Vo, S. Wohlrab, *Langmuir* 18 (2002) 4263–4269;
(e) C.D. Vo, D. Kuckling, H.-J. Adler, M. Schönhoff, *Colloid Polym. Sci.* 280 (2002) 400–409.
- [9] S. Seiffert, W. Oppermann, K. Saalwächter, *Polymer* 48 (2007) 5599–5611.
- [10] G.O. Schenck, W. Hartmann, S.-P. Mannsfeld, W. Metzner, C.H. Krauch, *Chem. Ber.* 95 (1962) 1642–1647.
- [11] J. Put, F.C. De Schryver, *J. Am. Chem. Soc.* 95 (1973) 137–145.
- [12] C.W. Miller, E.S. Jönsson, C.E. Hoyle, K. Viswanathan, E.J. Valente, *J. Phys. Chem. B* 105 (2001) 2707–2717.
- [13] C.E. Hoyle, S.-C. Clark, E.S. Jönsson, K. Viswanathan, *Photochem. Photobiol. Sci.* 2 (2003) 1074–1079.
- [14] F. Morel, C. Decker, E.S. Jönsson, S.C. Clark, C.E. Hoyle, *Polymer* 40 (1999) 2447–2454.
- [15] (a) H. Wang, J. Wei, X. Jiang, J. Yin, *Polymer* 47 (2006) 4967–4975;
(b) H. Wang, Y. Shi, J. Wei, X. Jiang, J. Yin, *J. Appl. Polym. Sci.* 101 (2006) 2347–2354.
- [16] J. von Sonntag, I. Janovsky, S. Naumov, R. Mehnert, *Macromol. Chem. Phys.* 202 (2001) 1355–1360.
- [17] J. von Sonntag, W. Knolle, *J. Photochem. Photobiol. A: Chem.* 136 (2000) 133–139.
- [18] J. von Sonntag, W. Knolle, S. Naumov, R. Mehnert, *Chem. Eur. J.* 8 (2002) 4199–4209.
- [19] J. von Sonntag, PhD thesis, Universität Leipzig, 2000.
- [20] J. von Sonntag, I. Janovsky, S. Naumov, R. Mehnert, *Macromol. Chem. Phys.* 203 (2002) 580–585.
- [21] C. Reichardt, *Chem. Rev.* 94 (1994) 2319–2358.
- [22] (a) H. Görner, *Chem. Phys. Lett.* 282 (1998) 381–390;
(b) C. Schweitzer, Z. Mehrdad, A. Noll, E.W. Grabner, R. Schmidt, *J. Phys. Chem. A* 107 (2003) 2192–2198;
(c) C. Schweitzer, R. Schmidt, *Chem. Rev.* 103 (2003) 1685–1757.
- [23] I. Carmichael, G.L. Hug, *J. Phys. Ref. Data* 15 (1986) 1–250.
- [24] P. Pareek, PhD thesis, Technische Universität Dresden 2006, <http://nbn-resolving.de/urn:nbn:de:swb:14-1115623310082-44480>.
- [25] C.G. Hatchard, C.A. Parker, *Proc. R. Soc., Lond., Ser. A* 235 (1956) 518–536.
- [26] F. Wilkinson, W.P. Helman, A.B. Ross, *J. Phys. Chem. Ref. Data* 22 (1993) 113–262.